Articles

Interloop Contacts Modulate Ligand Cycling during Catalysis by *Escherichia coli* Dihydrofolate Reductase†

Grover Paul Miller,‡ Daphne C. Wahnon,‡ and Stephen J. Benkovic*

Department of Chemistry, The Pennsylvania State University, University Park, Pennsylvania 16802

Received July 11, 2000; Revised Manuscript Received November 14, 2000

ABSTRACT: As a continuation to our studies on the importance of interloop interactions in the *Escherichia coli* DHFR catalytic cycle, we have investigated the role of the βG−βH loop in modulating the closed and occluded conformations of the Met20 loop during the DHFR catalytic cycle. Specifically, to assess the importance of the hydrogen bond formed between Ser148 in the βG−βH loop and the Met20 loop, Ser148 was independently substituted with aspartic acid, alanine, and lysine. Moreover, the βG−βH loop was deleted entirely to yield the Δ(146−148) DHFR mutant. Steady-state turnover rates for all mutants were at most 3-fold lower than the wild-type rate. Lack of an isotope effect on this rate indicated the chemistry step does not contribute to the steady-state turnover. Consistent with this finding, hydride transfer rates for the DHFR mutants were at least 10-fold greater than the observed steady-state rates. The values ranged from a 30% decrease (Ser148Ala and Ser148Lys) to a 50% increase (Ser148Asp) in rate relative to that of the wild type. Modifications of the βG−βH loop enhanced the affinity for the cofactor and decreased the affinity for pterin, as determined by the K_D values of the mutant proteins. Further analysis of Ser148Ala and Δ(146−148) DHFRs indicated these effects were manifest mainly in ligand off rates, although in some cases the on rate was affected. The Ser148Asp and Δ(146−148) mutations perturbed the preferred catalytic cycle through the introduction of branching at key intermediates. Rather than following the single WT pathway which involves loss of $NADP^+$ and rebinding of NADPH to precede loss of the product H4F (negative cooperativity), the mutants can reenter the catalytic cycle through different pathways. These findings suggest that the role of the interloop interaction between the βG−βH loop and the Met20 loop is to modulate ligand off rates allowing for proper cycling through the preferred kinetic pathway.

Dihydrofolate reductase (5,6,7,8-tetrahydrofolate:$NADP^+$ oxidoreductase, EC 1.5.1.3; DHFR)[1] catalyzes the reduction of 7,8-dihydrofolate (H_2F) to 5,6,7,8-tetrahydrofolate (H_4F) using nicotinamide adenine dinucleotide phosphate (NADPH) as a cofactor. As observed for many enzymes, catalysis by *Escherichia coli* dihydrofolate reductase is limited by physical rather than chemical processes (*1*). At pH 7.0, the flux of substrate through the DHFR catalytic cycle is limited by product release rather than by the rate of hydride transfer. Unlike eukaryotic cells, where the concentration of $NADP^+$ is no more than 1% of that of NADPH, prokaryotic cells have comparable levels of $NADP^+$ and NADPH (*2*). To reduce the level of product inhibition due to high $NADP^+$ concentrations, *E. coli* DHFR has evolved a catalytic cycle, which relies on binding of NADPH to accelerate product (H_4F) release. Ultimately, DHFR cycles through five kinetically observable intermediates to complete one catalytic cycle (*3*). Recent studies on DHFR have highlighted the inherent structural flexibility of the enzyme. As mapped by a series of X-ray crystal structures thought to mimic turnover complexes, loop movement and rotation between the two subdomains are the major elements that underlie the conformational flexibility of DHFR, and serve the critical role of determining the preferred kinetic pathway of the catalytic cycle (*4*). In particular, it has been suggested that loop movement is related to the evolutionary adaptation of *E. coli* DHFR to its $NADP^+$ rich environment.

As the DHFR subdomains rotate between open and closed states, the Met20 loop adopts one of two ligand-dependent conformations, closed or occluded. The distinction between the two Met20 loop conformations relates to the folding and positioning of residues Glu17−Met20 in the center of the loop and to the nature of the hydrogen bonding interactions with cofactor and adjacent loops. In the closed conformation

† This work was supported in part by NIH Grant GM24129. G.P.M. is the recipient of the Homer F. Braddock College of Science Memorial Scholarship.

* To whom correspondence should be addressed. Telephone: (814) 865-2882. Fax: (814) 865-2973. E-mail: sjb1@psu.edu.

‡ These authors contributed equally to this work.

[1] Abbreviations: DHFR, dihydrofolate reductase; Mtx, methotrexate; H_2F, 7,8-dihydrofolate; H_4F, 5,6,7,8-tetrahydrofolate; NADPH and NH, reduced nicotinamide adenine dinucleotide phosphate; NADPD, [4′-(*R*)-^{2}H]NADPH; DNADPH, 5,6-dihydro-NADPH; $NADP^+$ and N^+, oxidized nicotinamide adenine dinucleotide phosphate; EDTA, ethylenediaminetetraacetic acid; DTT, dithiothreitol.

10.1021/bi001608n CCC: $20.00
Published on Web 01/06/2001

observed in the substrate−cofactor complexes (DHFR·NADPH and DHFR·H_2F·NADPH), the central portion of the Met20 loop forms a short antiparallel sheet and type III′ hairpin turn, which mediates contacts with the nicotinamide ring of the cofactor. Although most of the hydrogen bond contacts with the Met20 loop involve backbone−backbone interactions, a notable exception is the contact between Asp122 (Oϵ2) of the βF−βG loop and the amide backbone of Glu17. After hydride transfer occurs between NADPH and dihydrofolate, the conformational equilibrium of the Met20 loop shifts to favor the occluded conformation. The hydrogen bonds between the N-terminal portion of the Met20 and βF−βG loops are disrupted, and new hydrogen bonds form between the Met20 and βG−βH loops involving Ser148 and the amide backbone of Asn23. Interestingly, Ser148 acts as both a hydrogen bond donor and acceptor to pin down the Met20 loop. The occluded Met20 loop conformation is observed in product tetrahydrofolate complexes (DHFR·H_4F·$NADP^+$, DHFR·H_4F, and DHFR·H_4F·NADPH), as well as the binary dihydrofolate complex (DHFR·H_2F). These observations can be viewed in terms of a thermodynamic equilibrium between the closed and occluded conformations that shift in response to ligand binding.

To assess the importance of the outer loops in stabilizing Met20 loop conformations, interloop contacts unique to the closed and occluded conformations were targeted for mutagenesis. For example, Asp122 of the βF−βG loop was substituted with asparagine, serine, and alanine, residues with successively less ability to form a hydrogen bond between Asp122 and the backbone amide of Glu17 observed in the closed Met20 loop conformation (*5*). Analyses of the Asp122 DHFR mutants enabled the construction of kinetic schemes at pH 7.0 that demonstrated two striking features. First, a significant correlation existed between the decreased level of NADPH binding and decreased hydride transfer rates resulting from these mutations. In other words, the interactions of Asp122 are along the reaction coordinate leading to the transition state. Second, substitutions for Asp122 alter the catalytic pathway preferred by wild-type DHFR under saturating conditions of the substrate and cofactor. Overall, the steady-state rate contains contributions from the product off rates from the DHFR·H_4F and DHFR·NADPH·H_4F complexes and from the rate of hydride transfer. These mutational effects confirmed a role of the βF−βG loop in stabilizing the closed conformation of the Met20 loop, whose importance in cofactor binding and in the formation of the appropriate Michaelis complex are underscored by the magnitude of these effects.

The deletion of Gly121 in the βF−βG loop produced a more dramatic effect on catalysis by DHFR (*6*, *7*). The goal of this study was the removal of a residue, which demonstrated nanosecond fluctuations in the binary folate complex (*8*) indicative of a highly flexible element within the βF−βG loop. Relative to the wild type, the deletion of Gly121 (ΔG121) decreased the rate of hydride transfer 550-fold and the strength of cofactor binding 20-fold for NADPH and 7-fold for $NADP^+$. Furthermore, ΔG121 DHFR required conformational changes that were dependent on the initial binary complex to attain the Michaelis complex poised for hydride transfer. Surprisingly, the insertion of glycine at the base of the modified βF−βG loop decreased the levels of both cofactor and pterin binding by a factor of 10. However,

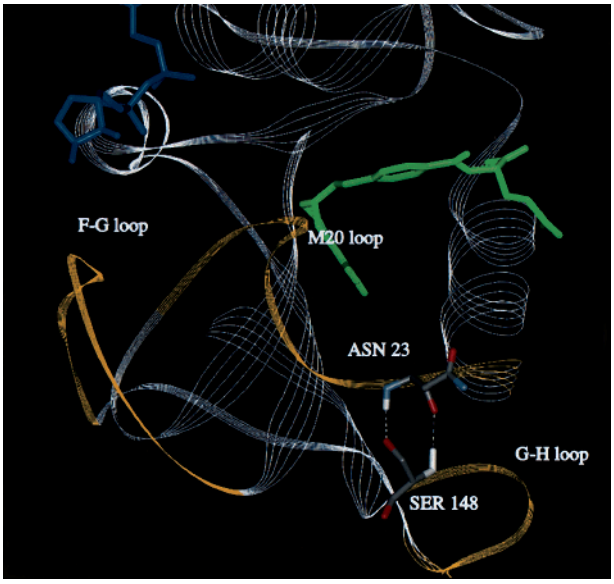

FIGURE 1: Hydrogen bonds between Ser148 and Asn23 stabilizing the occluded conformation.

the additional glycine eliminated conformational changes required by ΔG121 DHFR to attain the Michaelis complex. In other words, the length and register of the βF−βG loop are important for effective management of Met20 loop conformations by this loop.

As a complement to those studies, we constructed a series of mutants of the βG−βH loop purportedly involved in stabilizing the occluded Met20 loop conformation and characterized them kinetically. To assess the importance of the hydrogen bond formed between the hydroxyl group of Ser148 in the βG−βH loop and the amide backbone of Asn23 in the Met20 loop (Figure 1), Ser148 was independently substituted with aspartic acid, alanine, and lysine. The βG−βH loop was also deleted entirely to yield the Δ(146−148) DHFR mutant. Our mutations were designed to either strengthen or remove the stabilizing interactions in the occluded Met20 loop conformation. If the equilibrium model between the closed and occluded conformations is correct, mutation of serine to aspartic acid should further shift the equilibrium in favor of the occluded conformation through a charged-dipole interaction. In contrast, the Ser148Ala substitution should eliminate the bond stabilizing the occluded conformation, and destabilize this conformation shifting the equilibrium to the closed conformation. Like serine, lysine has the ability to form hydrogen bond donor−acceptor pairs; nevertheless, the substitution of Ser148 with lysine displaces the prospective hydrogen-bonding group (the amino terminus) by three methylene carbons relative to the wild-type serine residue. In the lysine Ser148L mutant, the likelihood of a strong hydrogen bond interaction between the βG−βH and Met20 loops would be decreased. We have analyzed the mutants for their effect on the thermodynamic and kinetic binding of the cofactor or pterin to the enzyme as well as for their effect on steady-state and pre-steady-state kinetic parameters. The Ser148Ala and Δ(146−148) DHFR mutants, in particular, were characterized more extensively.

MATERIALS AND METHODS

Materials. All reagents were purchased from Fisher Scientific or Sigma Chemical. Propagation of plasmid DNA

Table 1: Primers for Site-Directed Mutagenesis of the DHFR Gene[a]

primer	nucleotide sequence
DHFR-For	5′GCG GGA TCC CAT ATG ATC AGT CTG ATT GCG GCG3′
DHFR-S148A/D-For	5′GCG CAG AAC GA/CT CAT AGC TAT3′
DHFR-S148K-For	5′GCG CAG AAC AAG CAT AGC TAT3′
DHFR-Δ(146−148)-For	5′GAT GCT GAT GCG * CAT AGC TAT TGT3′
DHFR-Rev	5′GCG TCT AGA GGA TCC TTA ACG ACG CTC GAG GAT3′
DHFR-S148A/D-Rev	5′ATA GCT ATG AG/TC GTT CTG CGC3′
DHFR-S148K-Rev	5′ATA GCT ATG CTT GTT CTG CGC3′
DHFR-Δ(146−148)-Rev	5′ACA ATA GCT ATG * CGC ATC AGC ATC3′

[a] Asterisks indicate positions where the codons for amino acids 146−148 were deleted.

was carried out using *E. coli* DH5α cells. Restriction and DNA-modifying enzymes were purchased from New England Biolabs. Oligonucleotides for mutagenesis were synthesized on a 8909 Perceptive Biosystems DNA synthesizer. All assays were conducted in MTEN buffer {50 mM MES [2-(*N*-morpholino)ethanesulfonic acid], 25 mM Tris [tris-(hydroxymethyl)aminomethane], 25 mM ethanolamine, and 100 mM NaCl} at 25 °C. The pH of this buffer was adjusted to pH 7.0 or 9.0, depending on the design of the experiment.

Preparation of DHFR Ligands. The substrate, dihydrofolate (H_2F), was prepared from folic acid by dithionite reduction (*9*), whereas the product, (6*S*)-tetrahydrofolate (H_4F), was prepared from H_2F using *E. coli* dihydrofolate reductase (*10*). NADPH and $NADP^+$ were purchased from Sigma. The cofactor, [4′(*R*)-^{2}H]NADPH (NADPD), was prepared by using alcohol dehydrogenase from *Thermoanerobium brokii* and 2-propanol-d_8 to reduce $NADP^+$ as described by Viola and co-workers (*11*). Synthesis of 5,6-dihydro-NADPH (DNADPH) was accomplished by reduction of NADPH under 1 atm of hydrogen using a palladium−carbon catalyst (*12*). The following extinction coefficients were used to determine the concentrations of ligand solutions: 28 mM^{-1} cm^{-1} for H_2F at 282 nm and pH 7.4 (*13*), 28 mM^{-1} cm^{-1} for H_4F at 297 nm and pH 7.5 (*14*), 22.1 mM^{-1} cm^{-1} for MTX at 302 nm in 0.1 M KOH (*15*), 6.22 mM^{-1} cm^{-1} for NADPH (NADPD) at 340 nm and pH 7.0 (*16*), 18 mM^{-1} cm^{-1} for $NADP^+$ at 259 nm and pH 7.0 (*16*), and 18 mM^{-1} cm^{-1} for DNADPH at 259 nm and pH 7.0 (H.-g. Park, personal communication).

Construction of Mutant DHFRs. Standard DNA procedures were followed as described previously (*17*). The overlap extension technique was employed to substitute Ser148 with aspartic acid, alanine, and lysine and to generate Δ(146−148) (*18*). The expression plasmid, pET22b-DHFR (provided courteously by C. E. Cameron), was used as a template for the first polymerase chain reaction (PCR). Relevant primers are listed in Table 1. In brief, two independent PCRs were conducted: one reaction with the DHFR-For and the mutagenic reverse primers and the other reaction with the mutagenic forward and DHFR-Rev primers. The resulting products were gel purified and then used in a subsequent amplification employing the DHFR-For and DHFR-Rev primers. The desired expression construct was obtained by restriction digestion of the mutant gene with *Cla*I and *Bam*HI and then ligation into the pET22b-DHFR vector. Sequencing of plasmid DNA to confirm the presence of the desired mutations was performed by the Nucleic Acids Facility at The Pennsylvania State University.

Enzyme Purification. Wild-type and mutant DHFRs were purified as described previously (*7*). The production of dihydrofolate reductase (DHFR) utilized *E. coli* strain BL21-(DE3) cells transformed with the pET-22b-derived expression plasmid. Cells containing the pET22b-derived expression vector were grown at 37 °C to an OD_{600} of 0.8 in NCZYM medium (Gibco-BRL) containing 200 μg/mL ampicillin and induced with 0.4 mM IPTG. After induction for 4−6 h at 37 °C, the cells were harvested by centrifugation at 4 °C. From the cell pellet, a lysate was prepared and loaded on a methotrexate−agarose column (Sigma). Bound DHFR was eluted with folate at pH 9. To remove the folate from the eluant, the mixture was loaded on a DE-52 column and eluted using a 50 to 500 mM NaCl gradient, which effectively separated the DHFR from the folate (Whatman). DHFR was quantitated spectrophotometrically ($\epsilon_{280} = 0.0746$ μM^{-1} cm^{-1}) and by active site titration with MTX (*19*). Values obtained with these methods were within 10%.

Equilibrium Dissociation Constants. The dissociation constant, K_D, was measured by quenching of intrinsic protein fluorescence as a function of titrant concentration using an SLM Aminco 8000 (SLM Aminco Instruments, Inc.) or a Flouromax-2 (SA Instruments, Inc.) spectrofluorometer. Typically, DHFR was added to filtered, degassed MTEN buffer at pH 7.0 in a fluorescence cuvette. Tryptophan fluorescence was monitored at 340 nm from excitation at 290 nm. The addition of titrant decreased enzyme fluorescence. After correction for inner filter effects, the data were fit to a quadratic equation (*20*). Acceptable K_D determinations were made using enzyme concentrations that were lower than the respective K_D value. To quantitate DHFR, the active site was titrated with MTX using fluorescence quenching as stated above. If the protein concentration exceeds the K_D value for the ligand by 10-fold, a monotonic decrease in fluorescence will be observed until the active site is saturated. A fit of these data yields the concentration of active DHFR. All binding studies were performed at pH 7.0.

Steady-State Kinetic Parameter. The rate of substrate turnover under saturating amounts of H_2F and NADPH was determined by monitoring the decrease in NADPH absorbance at 340 nm ($\epsilon_{340} = 0.0132$ μM^{-1} cm^{-1}), whereby the temperature was maintained at 25 °C using a water-jacketed cuvette holder. For a typical experiment, 10−20 nM enzyme was preincubated with NADPH to avoid hysteresis, and the reaction was initiated upon addition of H_2F. Concentrations of H_2F and NADPH were varied from 50 to 200 μM to ensure that the reaction conditions were saturating.

To assess the reverse reaction, the same signal at 340 nm was monitored except under these conditions NADPH is being produced. Due to the high instability of tetrahydrofolate, attempts were made to minimize contact of H_4F with oxygen, light, and temperatures greater than 4 °C (except

Table 2: K_D Values of Ligands for Wild-Type and Ser148 Mutant DHFRs at 25 °C in MTEN at pH 7.0

ligand	wild type[a]	Ser148Asp	Ser148Ala	Ser148Lys	Δ(146−148)
Mtx (μM)	<0.01	<0.01	<0.01	<0.01	<0.01
NADPH (μM)	0.33 ± 0.06	0.15 ± 0.01	0.049 ± 0.003	0.16 ± 0.01	0.26 ± 0.03
$NADP^+$ (μM)	22 ± 4	10.9 ± 0.7	12 ± 1	10.3 ± 0.8	20 ± 3
H_2F (μM)	0.22 ± 0.06	0.18 ± 0.02	1.06 ± 0.09	0.72 ± 0.14	1.9 ± 0.3
H_4F (μM)	0.10 ± 0.01	0.12 ± 0.01	0.78 ± 0.12	1.1 ± 0.2	0.13 ± 0.02

[a] Taken from Fierke et al. (*3*).

Table 3: Kinetics of Ligand Binding for Wild-Type and Ser148 Mutant DHFRs at 25 °C in MTEN at pH 7.0

	wild type[a]		Ser148Ala		Δ(146−148)	
ligand	k_{on} (μM^{-1} s^{-1})	k_{off} (s^{-1})	k_{on} (μM^{-1} s^{-1})	k_{off} (s^{-1})	k_{on} (μM^{-1} s^{-1})	k_{off} (s^{-1})
NADPH	20 ± 1	3.5 ± 0.15	14 ± 1	<1	21 ± 1	69 ± 10
$NADP^+$	13 ± 3	300 ± 30	15 ± 1	100 ± 3	NA[b]	NA[b]
H_2F	42 ± 2	47 ± 10	27 ± 3	140 ± 20	7.9 ± 0.7	63 ± 9
H_4F	24 ± 1	<1	44 ± 3	41 ± 11	14 ± 1	30 ± 4

[a] Taken from Fierke et al. (*3*). [b] Not available due to the lack of an observable signal.

during assays). As a precaution, 5 mM DTT was added to all solutions. For a typical experiment, enzyme (0.1 μM) was preincubated with 2 mM $NADP^+$, and the reaction was initiated upon addition of 100 μM H_4F. Ligand concentrations were varied to ensure saturation of the enzyme.

Transient Kinetics. Transient binding and pre-steady-state kinetic experiments were performed on a stopped-flow instrument (Applied Photophysics Ltd.). Ligand binding and competition rates were measured by following quenching of the intrinsic enzyme fluorescence. Enzyme tryptophans were excited at 290 nm, resulting in fluorescence at 340 nm through a 305 nm output filter. The addition of ligand quenched the fluorescence, resulting in the measured signal. The designs of these experiments were based on principles discussed elsewhere (*3*, *21*, *22*). Pre-steady-state rates were measured by monitoring coenzyme fluorescence at 450 nm through a 400 nm output filter. This technique relies on excitation of enzyme tryptophans at 290 nm which subsequently emit at 340 nm, the absorbance band for the nicotinamide ring of the reduced cofactor. In a typical burst experiment, DHFR (3 μM) was preincubated with a saturating amount of NADPH (100 μM) in MTEN at pH 7.0 and 25 °C. The addition of a saturating amount of H_2F (100 μM) resulted in a burst followed by a linear phase, which could be fit to a single-exponential burst and a linear regression. The use of NADPD as a cofactor resulted in an isotope effect on the single-exponential rate, the chemistry step, of 2.8−3.0. Differences in the experimental designs for the mutants are discussed in detail in the Results and the Discussion.

RESULTS

Protein Expression and Purification. All of the DHFR mutants of the βG−βH loop were subcloned in a derivative of the pET22b plasmid (Novagen). The mutant proteins were expressed at a level of 2−6 mg/L of culture after a 4−6 h induction and purified to homogeneity. All enzymes bound the methotrexate−agarose column with high affinity, requiring folate to release the protein. No alteration of the purification protocol was required to obtain the final purity of the enzyme.

Thermodynamic Binding of Ligands. As described in Materials and Methods, the thermodynamic equilibrium dissociation constant (K_D) for each ligand was determined by monitoring the quenching of intrinsic fluorescence as a function of ligand concentration. These results are summarized in Table 2. All mutations of the DHFR βG−βH loop affected binding of the cofactor, pterin, or both. The Ser148Asp DHFR mutant displayed a 2-fold higher affinity for both oxidized and reduced cofactor and had no effect on pterin binding. The substitution of Ser148 with alanine enhanced the affinity for the cofactor, 6-fold for the reduced form and 2-fold for the oxidized form, at the expense of pterin binding, the level of which dropped 5-fold for H_2F and 8-fold for H_4F. In a similar fashion, the Ser148Lys DHFR mutant exhibited a higher level of binding for the cofactor, a 2-fold increase for both forms, and a lower level of binding for pterin, a 3.5-fold decrease for H_2F and a 10-fold decrease for H_4F. Surprisingly, loss of the βG−βH loop by deletion of residues 146−148 produced a less dramatic effect on binding than the substitution of Ser148 with alanine and lysine. Only the affinity for dihydrofolate was affected by this mutation. This mutation produced a dramatic 10-fold loss in substrate H_2F affinity without affecting product H_4F binding. Cofactor binding did not change as a result of the deletion of the βG−βH loop.

Relaxation Method of Binding Kinetics. The equilibrium constant reflects the balance between free and bound ligand, as the molecule binds and dissociates from the enzyme. To understand the nature of the mutational effects on the ligand K_D values, the binding kinetics for the respective ligands were determined employing the relaxation method for the Ser148 and Δ(146−148) DHFR mutants (*3*, *22*, *23*). These rates were determined for the formation of binding complexes for both substrates (NADPH and H_2F) and products ($NADP^+$ and H_4F) and are summarized in Table 3.

The substitution of alanine for Ser148 significantly affected the off rates of ligands, yet mildly affected their respective on rates. Both cofactor off rates deceased about 3-fold, whereas the pterin off rates increased 3-fold for H_2F and 40-fold for H_4F. The on rate for dihydrofolate decreased slightly, whereas the on rate for tetrahydrofolate increased approximately 2-fold. For the Δ(146−148) DHFR mutant, the most significant changes relative to the wild-type values were observed in the k_{off} values. The off rate for the reduced

Table 4: Ligand k_{off} Values from Wild-Type and Ser148 Mutant DHFR Complexes at 25 °C in MTEN at pH 7.0

ligand	enzyme species	trap	wild type[a] k_{off} (s^{-1})	Ser148Ala k_{off} (s^{-1})	Δ(146−148) k_{off} (s^{-1})
NADPH	DHFR·NADPH	$NADP^+$	3.6 ± 0.5	4.8 ± 0.4	16 ± 3
	DHFR·H_4F·NADPH		85 ± 10	27 ± 2	150 ± 8
	DHFR·folate·NADPH		8.4 ± 0.8	2.0 ± 0.2	8.6 ± 0.1
$NADP^+$	DHFR·$NADP^+$	NADPH	290 ± 20	28 ± 1	94 ± 6
	DHFR·H_4F·$NADP^+$		200 ± 20	93 ± 3	120 ± 6
	DHFR·H_2F·$NADP^+$		50 ± 10	36 ± 5	40 ± 1
H_2F	DHFR·H_2F	Mtx	22 ± 5	72 ± 3	92 ± 6
	DHFR·H_2F·DNADPH		20.0 ± 0.5	220 ± 10	260 ± 18
	DHFR·H_2F·$NADP^+$		6.6 ± 1	4.4 ± 0.4	NA[b]
H_4F	DHFR·H_4F	Mtx	1.4 ± 0.2	32 ± 1	37 ± 2
	DHFR·H_4F·NADPH		12 ± 2	113 ± 2	87 ± 2
	DHFR·H_4F·$NADP^+$		2.4 ± 0.2	36 ± 3	34 ± 1

[a] Taken from Fierke et al. (*3*). [b] Not available due to the lack of an observable signal.

Scheme 1

$$E{\bullet}L_1 \underset{k_1}{\overset{k_{-1}}{\rightleftharpoons}} E + L_1$$

$$E + L_2 \underset{k_{-2}}{\overset{k_2}{\rightleftharpoons}} E{\bullet}L_2$$

cofactor (NADPH) increased 20-fold, and the on rate was not affected by the mutation. The binding kinetics for $NADP^+$ could not be determined accurately due to a low amplitude for the expected signal. Decreases of 5- and 2-fold were observed in the on rate of H_2F and H_4F, respectively. The off rates showed an increase of 50% for H_2F and 30-fold for H_4F relative to that of the wild type. In the case of dihydrofolate, the on rate is affected more than the off rate, which is the opposite trend observed for tetrahydrolate binding. The K_D values calculated from the k_{off}/k_{on} rates for the various ligands to both Ser148Ala and Δ(146−148) are within a factor of 5 and showed no systematic trend. The calculated K_D of H_4F as a ligand to Δ(146−148), however, is 16-fold lower than the measured K_D.

Dissociation Rate Constants for Ligands. As a complement to the former studies, the off rates of ligands from multiliganded complexes were determined for both the Ser148Ala and Δ(146−148) DHFR mutants, employing the competition method. These values are summarized in Table 4. In this technique (*3*, *24*), the enzyme−ligand complex ($E{\bullet}L_1$) is mixed with a large excess of a second ligand (L_2). The principle of this approach relies on the ability of the second ligand to compete for the primary ligand (L_1) site as shown in Scheme 1. When $k_1[L_1] \ll k_2[L_2] \gg k_{-1}$, k_{obs} is a measure of the dissociation off rate for L_1. The measured signal is the difference between the fluoresence quenching by the two ligands upon formation of their respective enzyme−ligand complexes. An advantage of this technique over the relaxation method is the ability to utilize high enzyme concentrations, which provides large signal amplitudes for rate determinations.

The k_{off} values for the liganded complexes of the Ser148Ala DHFR mutant demonstrated trends similar to the data obtained by the relaxation method; namely, cofactor off rates decreased for the most part, and the pterin off rates increased. Generally, the agreement between the two methods was within a factor of 2−3 with the exception being the off rate for dissociation of NADPH from the DHFR−NADPH complexes which differed by more than 4-fold.

The changes in the off rates were dependent upon occupation of the adjacent binding site. In wild-type DHFR, the rate of dissociation of NADPH from the DHFR·H_4F·NADPH complex is 24-fold greater than the rate of dissociation from the binary complex. In contrast, the difference in these off rates for the Ser148Ala mutant is only 6-fold. The off rates for dissociation of $NADP^+$ from both the binary and ternary complexes of the Ser148Ala mutant are significantly slower than those observed in wild-type DHFR, where no significant difference in the $NADP^+$ off rate is observed upon occupation of the adjacent H_4F site. For the Ser148Ala mutant, the rate of dissociation of $NADP^+$ from the DHFR·H_4F·$NADP^+$ complex is 3-fold greater than from the binary DHFR·$NADP^+$ complex.

In the case of H_2F, the mutation had no effect on the dissociation from the ternary complex (DHFR·H_2F·$NADP^+$) but resulted in a significantly increased off rate of dissociation from the binary complex relative to that of the wild type. Interestingly, a large effect on the H_2F off rate was obtained from the analogue Michaelis complex, where dihydro-NADPH (DNADPH) was substituted for the reduced cofactor. Binding of DNADPH enhanced the H_2F off rate 10-fold relative to that of the wild type, as compared to at most a 3-fold effect on the other complexes. The rates of dissociation of tetrahydrofolate from the binary DHFR complex increased 23-fold relative to that of the wild type and were further increased in the presence of bound NADPH by 3−4-fold. Although the rates observed for Ser148Ala are faster than that of the wild type, the mutation attenuates the effect of the bound NADPH on the off rate of H_4F. In the wild type, the presence of NADPH increases the off rate of H_4F by 9-fold, whereas in the mutant, the increase is 3−4-fold. As observed in the wild type, the presence of bound $NADP^+$ did not produce a further increase in the H_4F off rate.

The differential effects of the βG−βH loop deletion on cofactor and pterin binding were also observed for the ligand off rates. The elevated off rates for pterin were similar to the effect of the Ser148Ala substitution, including the trend for the cofactor effects on pterin binding and dissociation from the analogue Michaelis complex. In contrast, the Δ(146−148) DHFR mutant displayed a different effect on cofactor off rates than the Ser148Ala DHFR mutation.

In the loop deletion mutant, the rate of dissociation of both the reduced and oxidized cofactor from their respective binary complexes was more significantly affected than the

Table 5: Steady-State Rates for Wild-Type and Ser148 Mutant DHFRs at 25 °C in MTEN at pH 7.0

parameter	wild type[a]	Ser148Asp	Ser148Ala	Ser148Lys	Δ(146−148)
k_{cat} (s^{-1})	12.3 ± 0.7	4.6 ± 0.1	6.6 ± 0.8	5.7 ± 0.1	14.5 ± 0.4
^{D}V	1.1 ± 0.1	1.10 ± 0.06	0.97 ± 0.12	1.03 ± 0.05	1.12 ± 0.02

[a] Taken from Fierke et al. (*3*).

Table 6: Pre-Steady-State Burst Rates for Wild-Type and Ser148 Mutant DHFRs at 25 °C in MTEN at pH 7.0

parameter	wild type[a]	Ser148Asp	Ser148Ala	Ser148Lys	Δ(146−148)
k_b (s^{-1})	220 ± 10	319 ± 2	157 ± 3	162 ± 2	206 ± 3
^{D}V	2.9 ± 0.2	3.0 ± 0.1	2.7 ± 0.1	3.2 ± 0.1	2.5 ± 0.1

[a] Taken from Fierke et al. (*3*).

Table 7: Steady-State Rates for Wild-Type and βG−βH Loop Mutant DHFRs at 25 °C in MTEN at pH 9.0

parameter	wild type	Ser148Asp	Ser148Ala	Ser148Lys	Δ(146−148)
forward k_{cat} (s^{-1})	3.0 ± 0.2	1.40 ± 0.03	1.48 ± 0.04	1.40 ± 0.03	2.2 ± 0.1
V_{for}	2.9 ± 0.2	1.7 ± 0.2	1.47 ± 0.07	1.8 ± 0.2	2.4 ± 0.1
reverse k_{cat} (s^{-1})	0.6 ± 0.1	0.44 ± 0.01	0.66 ± 0.04	0.52 ± 0.02	0.63 ± 0.01

rate of dissociation from the ternary complexes. The k_{off} value for NADPH increased 4-fold, and k_{off} for $NADP^+$ decreased 3-fold relative to the wild-type values in the binary complexes. The presence of bound pterin attenuated these effects to yield mutant off rates that varied less than 2-fold from the corresponding wild-type rates. The opposite effects of the βG−βH loop deletion on oxidized and reduced forms of cofactor differ from the trend to lower off rates observed for the Ser148Ala DHFR mutant.

Steady-State Kinetics. The steady-state rates (k_{cat}) of substrate turnover were determined for the mutant DHFRs and are summarized in Table 5. The substitution of Ser148 decreased k_{cat} values 2−3-fold, whereas the deletion of residues 146−148 did not affect the observed rate. To address a potential contribution of the hydride transfer rate to the observed rate, deuterated NADPH was employed as a cofactor. Under steady-state conditions at pH 7.0, the rate of substrate turnover by wild-type DHFR is the off rate of tetrahydrofolate from the mixed ternary complex (DHFR·NADPH·H_4F) (*3*). Since the rate of hydride transfer is much greater than k_{cat} (220 vs 12 s^{-1}), the deuterated cofactor does not affect the observed steady-state rate for wild-type DHFR. Analyses of the mutant DHFRs showed an isotope effect of approximately 1.0, indicating that a process other than chemistry is the rate-determining step.

Pre-Steady-State Kinetics. When hydride transfer is faster than the product off rate as for wild-type DHFR, a burst of product formation occurs prior to attaining the steady-state rate. This burst rate (k_b) is isotopically sensitive to deuterated NADPH, where $^{D}V = 2.8$. To determine if the βG−βH loop mutations affected the rate of chemistry, pre-steady-state experiments were performed for all mutant DHFRs. The k_b values and respective isotope effects are summarized in Table 6. Surprisingly, substitution of Ser148 with Asp increased the hydride transfer rate approximately 50%, whereas the lysine and alanine substitutions resulted in a 25% decrease for this rate relative to that of the wild type. Despite the binding effects and conformational change during NADPH binding, the deletion of residues 146−148 did not affect the chemical step.

Determining K_{eq} for Hydride Transfer. The hydride transfer step is pH-dependent, demonstrating a decrease in rate at higher pH. For wild-type DHFR, hydride transfer is rate-limiting at pH 9.0. The lower hydride transfer rate facilitates the determination of the reverse hydride transfer rate. Taken together, it is possible to calculate a K_{eq} value for the chemical step. This approach was applied to wild-type and βG−βH loop mutant DHFRs, and the results are summarized in Table 7. Unfortunately, the lack of a full isotope effect of 3.0 on the forward rates indicates that other rates, likely ligand off rates, contribute to the overall steady-state rate even at high pH.

Scheme 2: Kinetic Scheme for Ser148Ala DHFR at 25 °C in MTEN at pH 7.0[a,b]

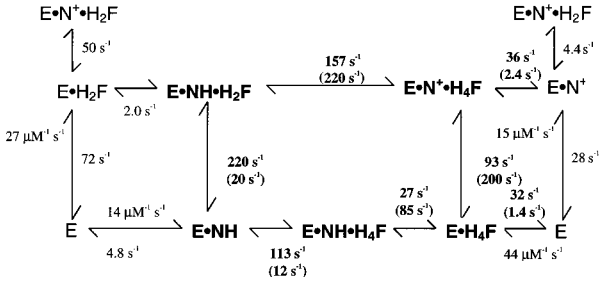

[a] NH is NADPH. N^+ is $NADP^+$. H_2F is dihydrofolate. H_4F is tetrahydrofolate. [b] For comparison, the values in parentheses denote the respective wild-type rates.

Summary of the Partial Kinetic Scheme. Determination of the ligand K_D values (Table 2), ligand binding kinetics (Tables 3 and 4), and rates of substrate conversion (Table 6) enables the construction of a partial kinetic scheme for the Ser148Ala and Δ(146−148) DHFR mutants at pH 7.0. For simplicity, only the partial kinetic scheme for Ser148Ala DHFR is shown (Scheme 2). The five intermediates observed in the wild-type cycle are shown in bold.

DISCUSSION

An intrinsic flexibility of protein structure is a key element in the function of many enzymes (*25*). For example, as observed for many other enzymes, catalysis by DHFR is limited by physical rather than chemical processes (*1*). As mapped by a series of X-ray crystal structures thought to mimic the five kinetically observed intermediates of the DHFR catalytic cycle, loop movement and rotation between

two subdomains are major elements that underlie the conformational flexibility of DHFR (*4*). These conformational changes serve a critical role in determining the preferred kinetic pathway for the DHFR catalytic cycle.

As a continuation of our studies of the role of interloop interactions in the DHFR catalytic cycle, we have investigated the role of the βG−βH loop in modulating the conformation of the Met20 loop during the DHFR catalytic cycle. Whereas the closed conformation involved mostly backbone−backbone hydrogen bonds between the βF−βG and Met20 loops, the occluded loop involves almost exclusively two hydrogen bonds between the hydroxyl group of Ser148 and the amide backbone of Asn23 (Figure 1). The smaller number of interactions would make the occluded conformation more sensitive to mutagenesis experiments. Since the occluded Met20 loop conformation is observed in product tetrahydrofolate complexes (DHFR·H_4F·$NADP^+$, DHFR·H_4F, and DHFR·H_4F·NADPH) and the closed conformation occurs in substrate complexes (DHFR·NADPH and DHFR·H_2F·NADPH), we would predict that destabilizing the occluded conformation and shifting the equilibrium to the closed conformation would result in an increase in the level of binding of substrates (H_2F and NADPH) and the disfavoring of product binding (H_4F and $NADP^+$). This study, however, has demonstrated that modifications of this loop interaction affect cofactor and pterin affinity primarily as distinct classes of ligands without distinguishing whether the molecule was a substrate or a product. Nevertheless, the more thorough investigation of Ser148Ala and Δ(146−148) catalysis indicated that the cycling of the enzyme under steady-state conditions no longer required negative cooperativity since the elevated pterin off rates and lowered cofactor off rates promote branching of the catalytic cycle through alternate intermediates.

To strengthen the interaction between the βG−βH and Met20 loops thus favoring the occluded conformation, we substituted Ser148 with aspartic acid. This mutation had little effect on cofactor or pterin binding. A 2-fold enhancement of both NADPH and $NADP^+$ binding was observed. Although these results were unexpected, the observed changes were mild compared to the results of the other βG−βH loop mutants. The observation of aspartic acid in DHFR sequences from *Candida albicans* (*26*) and glutamic acid in *T. gondii* (*27*) and *E. faecium* (*28*) may indicate the equivalency of an acidic residue as a replacement for Ser148.

Loss of the hydrogen bond by substitution with alanine or lysine yielded mutant DHFRs that shifted affinity to favor cofactor binding and disfavor pterin binding, as determined by the K_D values for the respective binary complexes (Table 2). Interestingly, the trend was more pronounced for the reduced cofactor over $NADP^+$ and tetrahydrofolate over dihydrofolate. A shift in the Met20 loop conformational equilibrium from occluded to closed is consistent with this finding. The closed conformation provides more binding interactions for NADPH than for $NADP^+$. In fact, the oxidized nicotinamide ring spends most of the time in solvent (*4*). Thus, favoring the closed conformation would result in not only a higher affinity for cofactor but also a more significant effect on the reduced form. A similar preferential effect on binding is observed for the pterins. The loss in affinity for tetrahydrofolate was 3-fold greater than the loss in affinity for dihydrofolate. The higher sensitivity of H_4F binding versus H_2F binding to the Ser148 mutants of the βG−βH loop argues that the occluded conformation serves a more important role in binding product tetrahydrofolate over substrate dihydrofolate. Taken together, this trend indicates that the role of the occluded loop is to modulatethe affinity for NADPH and tetrahydrofolate, which would be to disfavor NADPH binding and favor tetrahydrofolate binding in accordance with the proposed conformational model. The overall higher affinity for the cofactor along with the lowered affinity for pterin also indicates a more basic role of this loop is to modulate contacts with these classes of compounds.

It seems reasonable that removal of the βG−βH loop (residues 146−148) would produce a more dramatic effect on thermodynamic equilibrium binding than substitution of Ser148 alone. Surprisingly, the Δ(146−148) DHFR mutant displayed K_D values for both reduced and oxidized cofactor within error of wild-type values, indicating the higher affinity gained by the removal of Ser148 may be offset by another structural effect on binding as a result of the deletion. Binding of H_2F was weakened by 10-fold, while the level of H_4F binding was within error of the wild-type value. The observed results may indicate that an important function of the βG−βH loop is to distinguish between the substrate (H_2F) and product (H_4F).

Whereas K_D values are informative with regard to thermodynamic equilibrium binding interactions, the flux of the substrate is ultimately determined by microscopic rate constants comprising the catalytic cycle. Since the alanine substitution induced the most pronounced effect on binding and the deletion mutant displayed rather unusual characteristics, we chose to determine the on and off rates of the cofactor and pterin for the Ser148Ala and Δ(146−148) DHFR mutants, respectively. The following discussion of off rates will be limited to the results obtained from competition experiments for two reasons. The relaxation method determines the kinetic constants for a rapid equilibrium of the ligand with the enzyme. The initial collision complex may not be the most thermodynamically stable and may require a conformational change following ligand binding. The true off rate for dissociation from the binary complex would in fact be reflected with the competition experiment. Another consideration with the relaxation method is that analysis is limited to a range of ligand concentrations that provide a measurable signal. With regard to the fit of the data set to a linear regression, the slope (k_{on}) is less sensitive to errors in the data than the *y*-intercept (k_{off}), and thus, a higher confidence is placed on the on rate than the off rate.

For Ser148Ala, the on rates varied by less than 2-fold from wild-type values. The most significant effect on the off rates was observed for loss of H_4F. The degree of loss of H_4F from the binary complex increased by 23-fold compared to that of the wild type, while the degree of loss of H_4F from the DHFR·H_4F·NADPH complex was nearly 10-fold greater. The effect of adjacent NADPH binding in the mutant is less drastic than in the wild type. The second significant affect on off rates occurs in the loss of $NADP^+$. The dissociation of $NADP^+$ in Ser148Ala is 10-fold slower than in the wild type. The presence of H_4F has a negligible effect on the $NADP^+$ off rate in the wild type, while in the mutant, occupation of the H_4F site produces a 3-fold increase in the

extent of $NADP^+$ dissociation, which still remains lower than the wild-type level.

DHFR cycles through five kinetically observable intermediates (shown in bold) in the preferred pathway. The cycling through this pathway is determined by the relative on and off rates of ligands from the intermediate complexes. The partial kinetic scheme for Ser148Ala is shown in Scheme 2. As a consequence of the Ser148Ala mutation, there is an uncoupling of the inner wild-type catalytic cycle (as indicated with bold arrows). Upon formation of the DHFR·H_4F·$NADP^+$ complex, Ser148Ala can partition to form either DHFR·$NADP^+$ or DHFR·H_4F. The ratio of off rates from these complexes has decreased from 83 (in favor of the DHFR·H_4F complex) in the wild type to 3 in the mutant, allowing the possibility of the reaction to leak away from the inner cycle through the DHFR·$NADP^+$ complex. In addition, the off rates for dissociation of H_4F from DHFR·H_4F·$NADP^+$ and DHFR·H_4F are comparable and similar to the off rate for dissociation of $NADP^+$ from DHFR·H_4F·$NADP^+$. Thus, the free enzyme may be regenerated by loss of H_4F followed by $NADP^+$ or vice versa. The net result is a loss of the preferred wild-type kinetic catalytic cycle, which now does not require the loss of $NADP^+$ to precede the loss of H_4F. In other words, the steady-state rate no longer reflects a single rate, such as H_4F loss from the DHFR·H_4F·NADPH complex. Rather, the observed rate consists of contributions from alternate pathways that lead back to the Michaelis complex through the DHFR·H_4F·$NADP^+$, DHFR·H_4F, and DHFR·H_4F·NADPH complexes.

Deletion of the βG−βH loop affects the dissociation of H_4F like it does the dissociation of Ser148Ala DHFR (Table 4). The magnitude of the H_4F off rates from both the binary and DHFR·H_4F·NADPH complexes has increased substantially relative to that of the wild type (26- and 7-fold, respectively). Bound NADPH enhances the mutagenic effect on k_{off} for H_4F relative to that of the wild type, 2- versus 8-fold, respectively. The dissociation of H_4F from the binary DHFR·H_4F complex occurs at a rate of 37 s^{-1} and increases by a factor of only 2 in the ternary DHFR·H_4F·NADPH complex. The deletion mutant is characterized by a decrease in the $NADP^+$ off rate that is smaller than that observed in Ser148Ala; i.e., the off rate for dissociation of $NADP^+$ from the both the binary DHFR·$NADP^+$ and tertiary DHFR·$NADP^+$·H_4F complex is reduced compared to that of the wild type. The changes in H_4F and $NADP^+$ dissociation rates lead to the same kinetic consequence as observed for Ser148Ala. Upon formation of the DHFR·H_4F·$NADP^+$ complex, this intermediate can partition to form either the DHFR·$NADP^+$ or DHFR·H_4F complex. The ratio of off rates from this complex has again decreased from 83 (in favor of the DHFR·H_4F complex) in the wild type to 3 in this mutant. Because the off rates for dissociation of H_4F from the DHFR·H_4F·$NADP^+$ and DHFR·H_4F complexes are comparable and competitive with the off rate for dissociation of $NADP^+$ from the DHFR·H_4F·$NADP^+$ complex, free enzyme may be regenerated through this pathway. Thus, although the thermodynamic equilibrium results for the deletion mutant were not very similar to those obtained for the Ser148Ala mutant, the changes in the binding kinetics exhibited similar trends.

The steady-state rates for substrate turnover by the βG−βH loop DHFR mutants were similar to the wild-type value (Table 5). No trend was apparent for these rates with respect to the mutations. The off rate for dissociation of H_4F from the mutant DHFR·H_4F·$NADP^+$ complex is substantially higher than that observed for the wild type; therefore, it is unlikely that the observed mutant steady-state rate is still primarily the off rate for dissociation of the product from this mixed ternary complex. The off rates for the Ser148Ala and Δ(146−148) mutants indicate that the evolutionary preference for negative cooperativity has been lost despite small changes in the observed steady-state rates relative to the wild-type rate. When deuterated NADPH is used as a cofactor, the isotope effect is approximately 1.0 for all DHFRs, indicating the rate of hydride transfer is not contributing to the turnover rate.

As determined by pre-steady-state experiments, alterations in the βG−βH loop did not appreciably affect the rate of hydride transfer, which was altered at most by 50% by these mutations. Even the deletion mutant performed chemistry within error of the wild-type value. It is unclear why the aspartate substitution of Ser148 enhanced the hydride transfer rate (50%), whereas the lysine and alanine substitutions slightly decreased this rate (<25%). This finding indicates the role of the βG−βH loop in the DHFR catalytic cycle does not lie along the reaction coordinant leading to the transition state. In contrast, substitutions of the βF−βG loop, which destabilized the closed Met20 loop conformation, decreased the hydride transfer rate by more than 25-fold relative to that of the wild type. This finding further substantiates the role of the occluded loop in modulating ligand affinity in DHFR catalysis.

A common feature of both Ser148Ala and Δ(146−148) DHFR mutants is the uncoupling of the catalytic cycle that typifies steady-state turnover by wild-type DHFR. Rather than cycling through the five intermediates shown in bold, both rapid tetrahydrofolate and lower $NADP^+$ off rates break the inner catalytic cycle by promoting the contributions of other enzyme−ligand complexes to the overall catalytic cycle. Unlike the exclusive role of Asp122 in the βF−βG loop as a modulator for two Met20 loop conformations, the βG−βH loop plays another more basic role providing stabilizing contacts, albeit indirectly, to enhance the affinity for pterin at the expense of cofactor binding. The mutant steady-state rates are influenced primarily by alterations in ligand affinity, namely, the dissociation rates for H_4F and $NADP^+$. This finding supports the role of the interloop interactions as modulators of optimal ligand cycling, a crucial component of the *E. coli* catalytic cycle adapted to a $NADP^+$ rich environment.

Concluding Remarks. In this study as well as in previous works (*5*−*7*), we have investigated the sensitive interplay of outer loops in guiding the function of the Met20 loop in DHFR catalysis. This complex system serves as an excellent model for structure−function studies in contrast to some reports, where a small loop is a simple, rigid lid interacting with a buried active site, such as inosine 5′-monophosphate dehydrogenase (*29*) and the well-characterized triosephosphate isomerase (*30*−*33*). As the number of novel enzymes increases each day, the evolved system of DHFR may describe a more common theme in other enzymatic mechanisms. Moreover, the evolutionary divergence between prokaryotic and vertebrate DHFRs involves the absence or presence of loops between secondary structure elements. Understanding the principles that underlie the function of

these loops could shed light on the catalytic potential of these classes of enzymes, namely, the ability of vertebrate DHFRs to reduce folate as well as dihydrofolate.

REFERENCES

1. Cleland, W. W. (1975) *Acc. Chem. Res. 8*, 145.
2. Appleman, J. R., Beard, W. A., Delcamp, T. J., Prendergast, N. J., Freisheim, J. H., and Blakely, R. L. (1990) *J. Biol. Chem. 265*, 2740−2748.
3. Fierke, C. A., Johnson, K. A., and Benkovic, S. J. (1987) *Biochemistry 26*, 4085−4092.
4. Sawaya, M. R., and Kraut, J. (1997) *Biochemistry 36*, 586−603.
5. Miller, G. P., and Benkovic, S. J. (1998) *Biochemistry 37*, 6336−6342.
6. Cameron, C. E., and Benkovic, S. J. (1997) *Biochemistry 36*, 15792−15800.
7. Miller, G. P., and Benkovic, S. J. (1998) *Biochemistry 37*, 6327−6335.
8. Epstein, D. M., Benkovic, S. J., and Wright, P. E. (1995) *Biochemistry 34*,
9. −11048.
10. Blakely, R. L. (1960) *Nature 188*, 231−232.
11. Mathews, C. K., and Huennekens, F. M. (1960) *J. Biol. Chem. 235*, 3304−3308.
12. Viola, R. E., Cook, P. F., and Cleland, W. W. (1979) *Anal. Biochem. 96*, 334−340.
13. Branlant, G., Eiler, B., and Biellmann, J. F. (1982) *Anal. Biochem. 125*, 264−268.
14. Dawson, R. M. C., Elliot, D. C., Elliot, W. H., and Jones, K. M. (1969) *Data for Biochemical Research*, p 199, Oxford University Press, Oxford, U.K.
15. Kallen, J. R., and Jenks, W. P. (1968) *J. Biol. Chem. 241*, 5845−5850.
16. Jeong, S.-S., and Gready, J. E. (1994) *Anal. Biochem. 221*, 273−277.
17. P.-L. Biochemicals (1961) *Circular OR-18*, Milwaukee, WI.
18. Sambrook, J., Fritsch, E. F., and Maniatus, T. (1989) *Molecular Cloning. A Laboratory Manual*, Cold Spring Harbor Laboratory Press, Cold Spring Harbor, NY.
19. McPherson, M. J., Quirke, P., and Taylor, G. R. (1991) *PCR: A Practical Approach*, Oxford University Press, Oxford, U.K.
20. Williams, J. W., Morrison, J. F., and Duggleby, R. G. (1979) *Biochemistry 18*, 2567−2573.
21. Taira, K., and Benkovic, S. J. (1988) *J. Med. Chem. 31*, 129−137.
22. Velick, S. F. (1958) *J. Biol. Chem. 233*, 1455−1467.
23. Dunn, S. M. J., and King, R. W. (1980) *Biochemistry 19*, 766−773.
24. Cayley, P. J., Dunn, S. M. J., and King, R. W. (1981) *Biochemistry 20*, 874−879.
25. Birdsall, B., Burgen, A. S., and Roberts, G. C. K. (1980) *Biochemistry 19*, 3723−3731.
26. Kempner, E. S. (1993) *FEBS Lett. 326*, 4−10.
27. Franceschi, M., Denaro, M., Irdani, T., Lorenzetti, R., Mastromei, G., Skarmoutsou, E., and Polsinelli, M. (1991) *FEMS Microbiol. Lett. 64*, 179−182.
28. Roos, D. S. (1993) *J. Biol. Chem. 268*, 6269−6280.
29. Gleisner, J. M., Peterson, D. L., and Blakley, R. L. (1974) *Proc. Natl. Acad. Sci. U.S.A. 71*, 3001−3005.
30. McMillan, F. M., Cahoon, M., White, A., Hedstrom, L., Petsko, G. A., and Ringe, D. (2000) *Biochemistry 39*, 4533−4542.
31. Lolis, E., Alber, T., Davenport, R. T., Rose, D., Hartman, F. C., and Petsko, G. A. (1990) *Biochemistry 29*, 6609−6618.
32. Lolis, E., and Petsko, G. A. (1990) *Biochemistry 29*, 6619−6625.
33. Kobayashi, N., Yamato, T., and Go, N. (1997) *Proteins 28*, 109−116.
34. Derreumaux, P., and Schlick, T. (1998) *Biophys. J. 74*, 72−81.

BI001608N